Proceedings World Geothermal Congress 2015
Melbourne, Australia, 19-25 April 2015

The Geothermal District Heating System on the Grado Island (North-Eastern Adriatic Sea)

Bruno Della Vedova*, Lorenzo Petronio+, Flavio Poletto+, Francesco Palmieri+, Alberto Marcon*, Piero Corubolo+, Biancamaria Farina+, Aurélie Cimolino*, Cinzia Bellezza+

*Dept. of Engineering and Architecture, Trieste University, Via Valerio, 10, I-34127 Trieste, Italy

+OGS (National Institute of Oceanography and Experimental Geophysics), Trieste, Italy

dellavedova@units.it

Keywords: district heating, geothermal doublet, low-enthalpy, carbonate reservoir, Grado Island, geophysical investigations, thermo-fluid-dynamic modeling

ABSTRACT

The feasibility of a geothermal district heating pilot-plant on Grado Island, northeastern Adriatic Sea (Italy), was the result of the *Grado geothermal Project, Phase 1*, completed in 2008 by the Regione Friuli Venezia Giulia, mostly supported by European Union funding. The reservoir characterization and the preliminary geothermal potential assessment rely on the geophysical prospect and on the exploration borehole drilled down to 1110 m. These investigations confirmed the existence of an untapped low-enthalpy geothermal reservoir within the Mesozoic carbonate platform buried beneath about 1 km of Paleogene and Neogene sediments, in correspondence of the structural highs along the coastal areas. The well production potential from a fossil, seawater confined aquifer, having a temperature of about 45-50 °C, was estimated to be about 140 tons/h.

In 2012, as part of the *Grado geothermal Project, Phase 2*, an integrated gravity and seismic geophysical prospecting, including multi-offset VSPs, was conducted in downtown Grado and in its surrounding lagoon. The target was to extend the investigation of the geothermal reservoir and to provide adequate information on the faults/fracture systems interesting the buried external Dinaric thrust front.

The results, here presented, allowed operators to locate the second well of the geothermal doublet, planned to feed the district heating system of public buildings on the island. The drilling of the second borehole is due by June 2014 and the deployment of the main distribution network by September 2014. Borehole geophysics, interference test measurements between the two wells located at distance of one km, and 3-D thermo-fluid dynamic numerical modeling will optimize the production and fluid re-injection and help to design the heat exchangers and to manage the sustainability of the geothermal plant.

1. INTRODUCTION

The structural highs of the foreland Mesozoic carbonate platform, buried beneath the lower Veneto and Friuli plains (NE Italy) and the north-Adriatic coastal areas, were characterized a few decades ago on the base of the available seismic, gravity and magnetic data, calibrated using borehole data of hydro-carbon exploration wells drilled on some structural culminations (e.g., AGIP, 1977, 1986, 1994; Cassano et al., 1986; Cati et al., 1987; Casero et al., 1990; Fantoni et al., 2002; Venturini, 2002; Fantoni et al., 2003; Nicolich et al., 2004). The Cesarolo-1 AGIP well, drilled on the Lignano-Cesarolo structural culmination, together with a large number of geothermal water wells in the upper sedimentary cover of the north-Adriatic coastal area (Barnaba, 2001; Grassi, 1994), and the new Grado-1 exploration borehole, reaching 1110 m of total depth (Della Vedova et al., 2008a,b; Cimolino et al., 2010), allowed to strengthen the conceptual model of heat transfer at depth by Bellani et al. (1994) and by Calore et al. (1995), supporting the positive geothermal anomaly in the area. In the Grado area, heat transfer by advection mainly occurs in the permeable and fractured carbonates of the buried outer Dinaric front thrust interested by anti-Dinaric strike-slip fault systems (Cimolino et al., 2010). Heat transfer by conduction prevails trough the low-permeability Cenozoic clastic deposits of the cover (Plio-Quaternary sequences, Lower Miocene terrigenous deposits, Oligo-Miocene Alpine Molasse, and Eocene Dinaric flysch).

The Regione Autonoma Friuli Venezia-Giulia, Servizio Geologico, carried out the first phase of the *Grado Geothermal Pilot Project*, supported by European funding 2000-2006. The results allowed (i) to understand the heat-transfer conceptual model in the area, (ii) to assess the geothermal potential of carbonate aquifer and, finally, (iii) to evaluate the feasibility of a district heating system, sustained by a production well and a re-injection well (Della Vedova et al., 2008a, b). The Grado-1 well was drilled in 2008 on the sand beach at the westernmost end of Grado Is., at about 100 m from the shoreline. The stratigraphic record shows 290 m of Plio-Pleistocene sediments, followed by 250 m of Neogene terrigenous successions and 50-60 m of Paleogene turbidites (Eocene flysch). The top of the Paleogene Nummulitic limestone shelf is at 616.5 m depth. The K-T boundary, found at 1007 m depth, is marked by a transition to Mesozoic (Upper Cretaceous) limestones, including a sedimentation *hiatus* and clear evidence of sub-aerial exposure and karstic phenomena (Cimolino et al., 2010). The drilling phase included three cores, well logs in the carbonate reservoir and pumping tests (Della Vedova et al., 2008a, b; Cimolino et al., 2010). The results show that the Paleogene and upper Cretaceous limestones exhibit open fractures and vugs containing salty warm waters with a temperature of 42-45 °C and an artesian flow rate of 0.028 m^3/s with a pressure of 280 kPa at wellhead. The core data and the acoustic and formation, neutron, porosity, gamma ray, and density logs, including a circumferential borehole imaging log (CBIL), provided detailed images of the fractures encountered by drilling, distributed with different patterns and orientations in the carbonate formations. The pumping tests indicated a sustainable production up to about 140 metric tons/h.

Given the positive results and the favorable conditions for the utilization of the low-temperature geothermal resources, the European Commission endorsed the second phase of the Grado Geothermal Project funding the Grado Municipality (POR-FESR 2007-2013 funding Program) to extend eastwards the geophysical survey, drill the second borehole and complete the surface

distribution network. The new geophysical survey investigated in detail the geometry, structures and physical properties of the carbonate geothermal reservoir and cap-rock units in the surrounding area of the Grado-1 well. The expected output is the characterization of the Paleogene-Upper Cretaceous limestones reservoir and the identification of the fault zones and thrust units that represent favorable hydraulic conditions for the hydrothermal circulation. The optimal performance of the geothermal doublet would require the average hydraulic transmissivity between the two well bottoms to be not too high, to avoid a hydraulic shortcut, and not too low, with the effect to preclude the closure of the hydrogeologic circulation system. The thrust and fault systems (still active) favor the fluids circulation and therefore their knowledge is crucial to characterize the geothermal reservoir and to locate the second borehole. For this purpose, we acquired an integrated surface and borehole seismic and gravimetric survey. In this paper we present the results of multichannel seismic reflection profiling combined with an accurate gravity investigation over a broader area, and the results of the borehole multi-offset vertical seismic profile (VSP), performed in the first exploration well (Grado-1) drilled in 2008 in the geothermal reservoir. VSP provide a strong link between the Grado-1 well logs and the surface reflection seismic acquisitions, including detailed seismic information in the well area and eastwards.

The aim of the integrated geophysical study was to improve the knowledge of the faulted area around the Grado-1 well, to provide data useful to estimate the location and extent of the fractured system, with the target to locate the second well of the geothermal system developed for district heating. The specific objectives of the VSP survey were to link borehole and surface seismic data, calibrate the new surface seismic data acquired for imaging purposes in the area surrounding the well, obtain high-resolution seismic information in depth, and in general measure the variations of the physical rock properties in the fractured carbonate formations encountered below 616,5 m depth at the well location. The borehole integrated approach provides additional and robust geophysical information for the numerical estimation of the fluid-dynamic modeling of the geothermal-doublet system, for reducing the drilling risk of the second well and for evaluating the optimal conditions for the sustainability of the geothermal system.

In this paper we present the results of multichannel seismic reflection profiling combined with an accurate gravity investigation over a broader area, and the results of the borehole multi-offset vertical seismic profile (VSP), performed in the first exploration well (Grado-1) drilled in 2008 in the geothermal reservoir. We also present the results of the preliminary numerical thermo-fluid dynamic simulations to support the drilling of the second well and the final design of the district heating system. The second borehole was advancing (by end of May 2014) into the Miocene molasse sediments (450 m depth).

2. GEOPHYSICAL SURVEY

2.1 Surface reflection seismic

The seismic reflection survey (Della Vedova et al., 2013) consists of energy shots and measurements acquired along three lines: G11, G12 and G13, which are 2.4, 2.6 and 2.4 km long, respectively (Fig. 1). Fixed-spread configuration with a trace interval of 10 m and six geophones (10 Hz natural frequency) per station, placed in a 10 m linear array, and 20 m shot interval was adopted. The source for G13 line was a seismic vibrator (IVI Minivib T-2500) operated with 2500 lbs peak force, 18 s linear upsweep (in the frequency range 8-200 Hz). The recording parameters included 1 ms sampling rate and 22 s of recording time. Geophone/hydrophone measurements, as well as Vibroseis pilot signals were acquired, correlated and stacked. Line G11 and line G12 have been shot with a Hydrapulse source (recording from 1 to 4 energizations per point) and with 1 ms sampling interval and 4 s listening time. Multichannel hydrophone bay-cable and offshore shots (by airgun - 80 cubic inches, 120 bars) were utilized to extend the onshore lines, and to increase the subsurface coverage and illumination at the end of the offshore line G11. Onshore shooting was performed during the night in order to limit the impact of the cultural noise on the data. In the most sensitive urban areas a vibration monitoring was accomplished. During the survey, the seismic source trucks (i.e., Minivib and Hydrapulse) were accompanied by Local Civil Protection and by the Municipal Police cars to maintain traffic control. For safety reason the offshore energizations were shot during daylight. The Summit DMT telemetric system supported the seismic data acquisition. A shot-by-shot quality control was performed during the seismic survey.

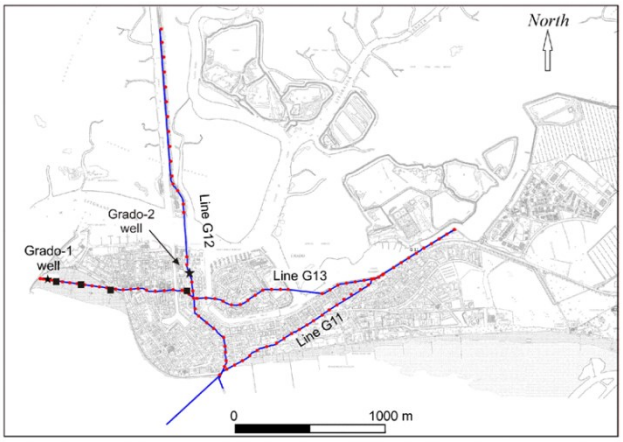

Figure 1: Location map of the surface seismic reflection survey (blue lines), of the Grado-1 VSP shot points (black squares) and of the gravity stations (red points) along the seismic lines. The black stars indicate the position of Grado-1 and Grado-2 wells.

The standard data processing sequence includes post-stack migration and time to depth conversion. The velocities obtained by the Grado-1 well near-offset VSP data (Poletto et al., 2013) were used to calibrate the time to depth conversion of surface seismic reflection data.

2.2 Borehole seismic survey

A multi-offset vertical seismic profile (VSP) survey consisting of four offset VSP's at different distances from the well, was acquired in the Grado-1 well to better characterize the area of the geothermal reservoir (Poletto et al., 2013). The total well depth is 1110 m. The borehole was completed with a steel-casing section, from surface down to 696 m depth, with the casing bottom end in the carbonate formation. The remaining well section down to total depth is open hole in fractured carbonates. In the deeper part, the well is characterized by drilling results. These measurements include three cores and conventional wireline logs, with acoustic and formation, neutron, porosity, gamma ray, and density logs. A circumferential borehole imaging log (CBIL) provides detailed images of the fractures encountered by the borehole, distributed with different patterns and orientation in the carbonate formations (Cimolino et al., 2010).

In this analysis we made different use of the near- and multi-offset borehole seismic information. A near-offset VSP was measured at a distance of 44 m from wellhead, with high-resolution parameters, using a 5 m depth sampling interval to characterize with high detail the seismic profile along the vertical well. Other three VSP were acquired at increasing distances of 226 m, 449 m and 939 m, with the objective to investigate the lateral structural features. These vertical profiles were acquired with larger depth intervals, of 10, 10 and 20 m, respectively. The offset VSPs were planned after evaluating the surface seismic data and the results of the near-offset VSP. In particular, the last VSP was acquired at a large offset of 939 m with the purpose of investigating the wavefield propagation in a complex fractured zone interpreted and expected at lateral side position with respect to the well. Due to logistic conditions encountered in the Grado island, the multi-offset VSPs were acquired by in-line positions of the source (accelerated dropping weight, Hydrapulse), along the direction of the line G13 of the surface reflection seismic survey crossing the exploration well and heading to the East (Della Vedova et al., 2013).

2.3 Gravity survey

A focused gravity investigation was conducted by the Trieste University starting from 1987 (Della Vedova et al., 1988) with a collection of a consistent dataset, tied to the gravity stations belonging to the Friuli microgravity network linked to the absolute gravity station in Trieste (Marson and Morelli, 1979). The same instrument *LaCoste&Romberg mod. D,* equipped with a feedback system to improve measurement quality, was used in the new survey. A total of 121 new gravity stations were acquired in the broad Grado area surrounding the reservoir structures, to increase the spatial coverage of the dataset collected in the eighties. Figure 2 shows the map with all the available gravity stations on Grado Is. and adjacent lagoon.

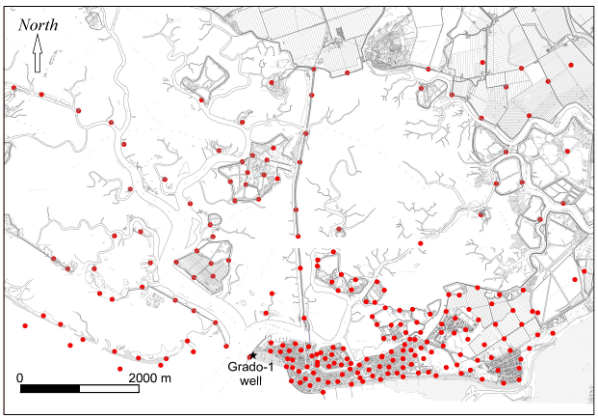

Figure 2: Gravity stations acquired on Grado Is. and adjacent lagoon (red points). The map includes some measurements acquired in 1987. The gravity measurements acquired along the seismic lines are located in Figure 1.

The gravity survey includes 108 other gravity measurements collected along the three seismic lines (Fig. 1), with an average space interval of 60 m. In the field data acquisition, we adopted the loop method to check both the drift term and the closure errors. These values were always less than ±0.005 mGal/h and ±0.005 mGal, respectively. The GPS Real Time Kinematics method provided the topographic control. All the gravity measurements were processed according to the standard procedures (Hinze et al., 2005); the theoretical g values were computed using the GRS80 formula, the Free Air correction using the formula that takes into account also the station latitude, the Bouguer correction with the Bullard B term, and the terrain correction, up to a radius of 10 km, with the right prism formula (Banerjee et al., 1977). The corrections were computed using a mass density of 2400 kg/m^3. Additional corrections were applied to compensate building effects for the measurements located downtown Grado city.

3. GEOPHYSICAL DATA RESULTS

3.1 Surface reflection seismic

Surface reflection and borehole seismic data were jointly interpreted starting from Grado-1 borehole stratigraphy. The interface between the terrigenous cap-rock sediments (Alpine Molasses and Paleogene Flysch) and the Paleogene carbonate geothermal reservoir is clearly detectable on the seismic sections; inside Paleogene carbonates two different facies (with lightly velocities changes) have been hypothesized. Figure 3 shows the seismic depth section G13 with the geologic interpretation (formations in coloured areas) for the main horizons (yellow lines) and some sub-vertical tectonic discontinuities (blue lines).

The top of geothermal reservoir is gently deepening (3-4°) to the North, as evidenced by line G12 (Fig. 4) and confirmed by the Bouguer anomaly gradient of 1.1 mGal/km.

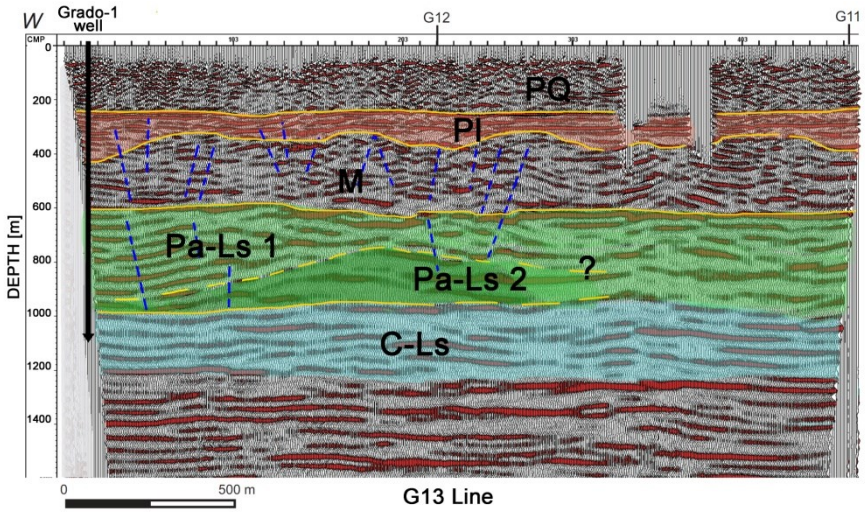

Figure 3: Multichannel seismic Line G13, with geologic interpretation. PQ (Plio-Quaternary loose sediments), Pl (Pliocene sediments), M (Molasses: alpine and Paleogene flysch), Pa-Ls (Paleogene Limestones: facies eteropy can be hypothesized), C-Ls (Upper Cretaceous Limestones).

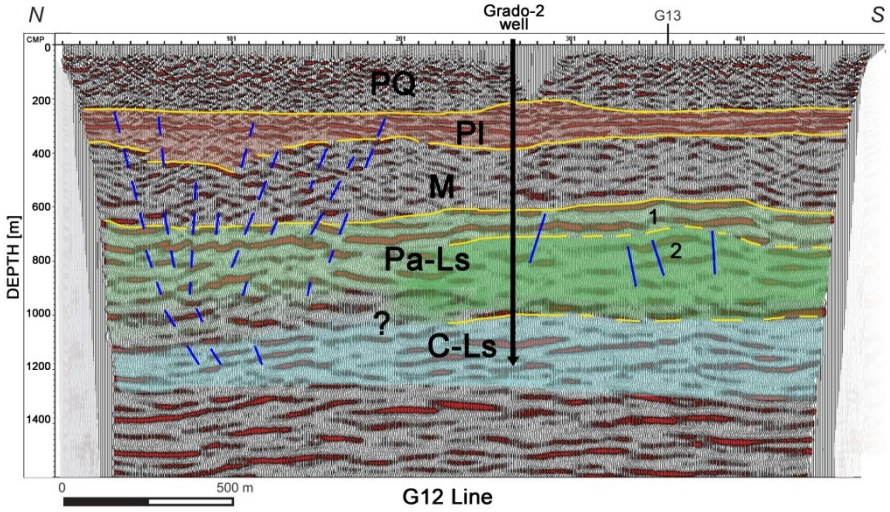

Figure 4: Multichannel seismic Line G12, with geologic interpretation. PQ (Plio-Quaternary loose sediments), Pl (Pliocene sediments), M (Molasses: alpine and Paleogene flysch), Pa-Ls (Paleogene Limestones: facies eteropy can be hypothesized), C-Ls (Upper Cretaceous Limestones).

The surface seismic images were integrated by VSP near offset and multi-offset results, which provide robust data to analyse formation properties. In the study area the Paleogene platform depth ranges from 600 to almost 70 m with a good lateral continuity. Locally some abrupt discontinuities of the seismic signal were interpreted as faults with relatively modest vertical displacement; the main active lineations seen on the surface seismic lines belong to the two main tectonic systems that characterize the distal Dinaric front: the frontal NW-SE direction thrusts and the anti-dinaric NE-SW direction transcurrent faults.

3.2 Near offset VSP

The near-offset VSP provides the link for seismic data to the high-resolution well logs and to the data of the borehole lithological profile. Figure 5a shows the high-quality total field of the near-offset VSP, vertical geophone (Z) component. Figure 5b shows the reflections in the two-way-time (TWT) deconvolved up-going signals after wavefield separation. These VSP seismic signals are of good quality and resolution, with frequency bandwidth extended up to 200 Hz. The TWT up-going wavefield is compared to the CBIL log and to the stratigraphic borehole profiles, represented in depth at the top of the VSP. The blue arrows indicate reflections interpreted as the transition from Neogene sediments to the top of the Paleogene carbonate platform at 616.5 m depth, the top of the geothermal reservoir, and the transition to the Mesozoic carbonates at 1007 m depth. The red arrows point to important sloping fractures, that were encountered while drilling the in the carbonate section immediately below the casing shoe, and, with different patterns of densely distributed fractures, in the deeper zone of the carbonate reservoir after 990 m depth.

This information greatly improves the detection and interpretation of the transition within the carbonate formation recognized by the surface reflection seismic. The interval velocity of the near-offset VSP was used for subsequent depth conversion of the surface

seismic data, i.e., for time-to-depth model calibration and depth migration to provide imaging and structural information at lateral well Grado-1 positions. Figure 6 shows the interval-velocity profile computed using the first breaks of the near-offset VSP of Figure 5a. We can observe significant velocity changes for compressional waves, in particular the sudden increase in the velocity at about 610 m depth that marks the top of the Paleogene carbonate platform.

The vertical VSP provides a depth calibration for the interpretation of the reflections in the surface seismic data. Figure 7 compares the near-offset VSP and the time section of the surface seismic survey G13 passing through the well Grado-1 (see Della Vedova et al., 2013). The formation changes can be interpreted in depth in the up-going VSP (Fig. 7a), where the depths of the transitions to and in the limestone platform are indicated by continuous vertical lines, and the corresponding seismic times are indicated by dashed horizontal lines. Figure 7c represents the transposed TWT VSP, plotted near and compared to a portion of the surface seismic section. The interpreted formation changes are clearly identified in the seismic section with the support of the VSP signal and velocity function.

For reservoir characterization purposes, a quality Q-factor analysis was performed using the near-offset VSP, in particular to study different attenuation zones between shallow and deep carbonate formations. Two approaches were used to estimate attenuation in the borehole formation. The first was based on the spectral-ratio method, which calculates the cumulative attenuation $B_{\bar{z}}$ between different depth intervals (Hauge, 1981), using the modified exponential approach proposed by Blias (2012). Figure 7c shows the cumulative attenuation profile obtained by the analysis of the separated down-going signals of the near-offset VSP. Higher attenuation with lower Q of the order of 20 was observed in the shallower alluvium zone. Lower attenuation with high Q factor of the order of 200 characterizes the carbonate formation at 0.55 s in the two-way-time (TWT) section, however with some variations in the deeper borehole section, at 0.65 s (lower carbonate platform) in the time section.This result is confirmed by the second approach for Q-factor analysis using the signals of very different frequency content of the available acoustic log and accurate measured travel-times in the near-offset VSP. We used the Kramers-Krönig relationship linking the velocity dispersion (velocity versus frequency relationship) and the attenuation for physical signals (Sun, Milkereit and Schmitt, 2009), using the velocities and frequencies of VSP and sonic logs. We report that the results confirm the good agreement between the VSP travel-time curve and the log integrated-time curve compensated by assuming Q = 200 for the correction of the dispersion in the limestone section.

All this information gives additional insight in the interpretation of the fractured reservoir properties in the proximity of the well Grado-1, which is also investigated from a structural and rock properties point of view with the support of the multi-offset data.

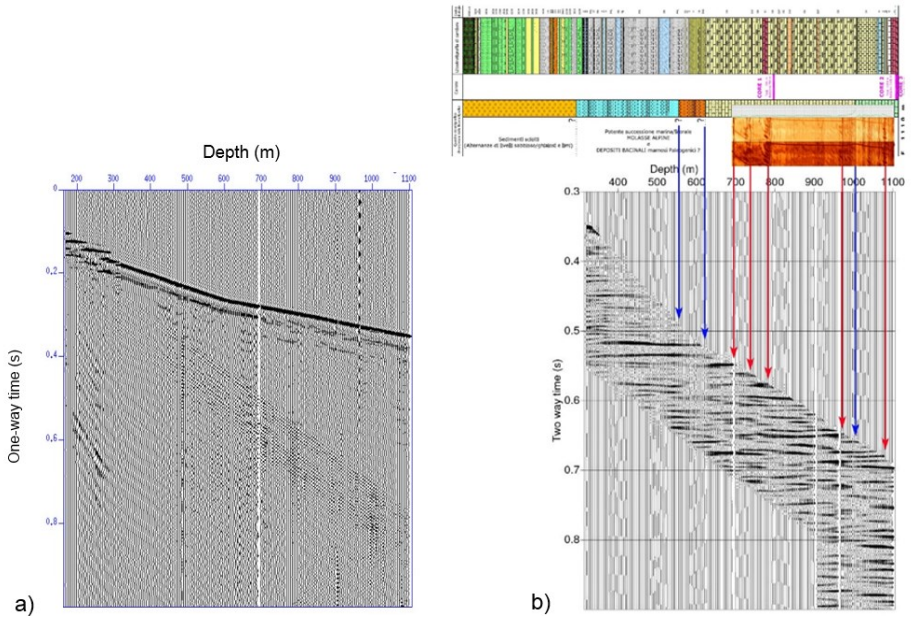

Figure 5: a) Total field of the near-offset VSP, Z geophone component. b) Separated TWT up-going reflection signal. Comparison between CBIL log, stratigraphic profile and VSP represented in depth at the top of the VSP. The correspondences between lithological changes, fractured zones and VSP signal are shown.

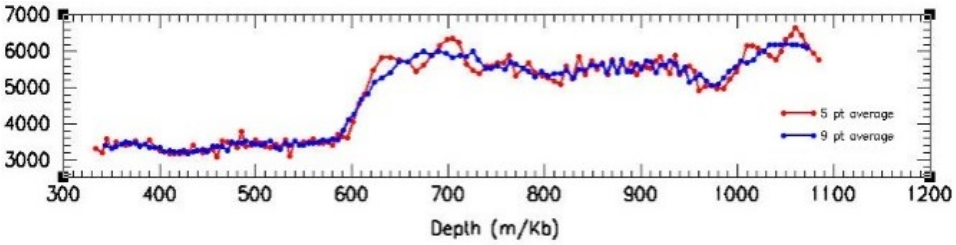

Figure 6: Velocity function calculated by picking the first break in the near-offset VSP. Data are averaged on 5 (red line) and 9 (blue line) points.

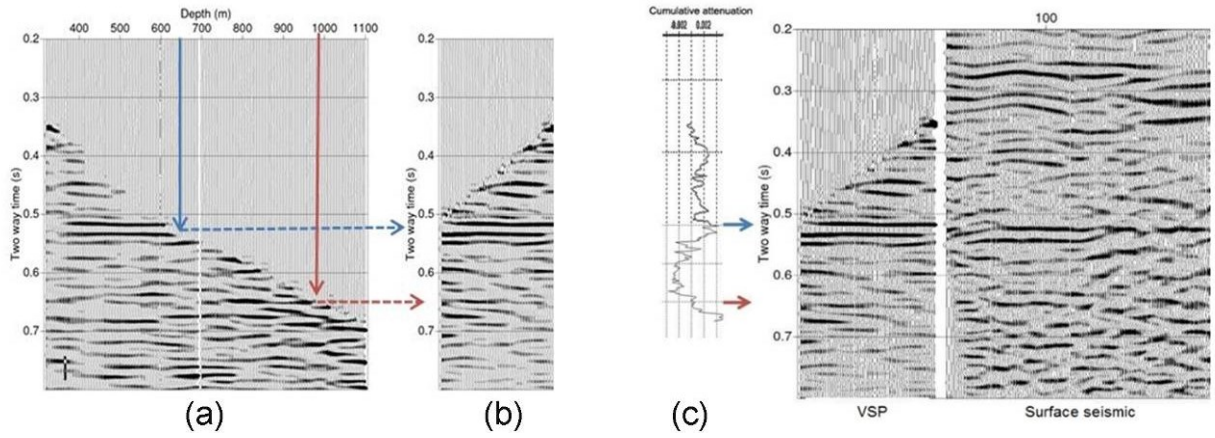

Figure 7: Correspondence between TWT near-offset VSP (a), transposed VSP (b), and a portion of the surface seismic line G13 passing through the well (c), with the cumulative attenuation analysis by spectral-ratio method, and reflection signal interpretation.

3.2 Multi-offset VSP

The multi-offset profile extends the analysis laterally with respect to Grado-1 well. Multi-offset data first breaks provided information about the velocity variation and structural features of the subsurface at lateral side positions below the surface seismic line G13 (Petronio et al., 2012; Della Vedova et al., 2013). To account for the proper wavefields, the VSP 3-component (3C) geophone signals measured with variable orientation at depth were rotated with angles calculated in a time window centred around compressional direct arrivals. Data rotation provides the radial R and the vertical-transverse T components starting from the recorded vertical and horizontal ones (Z, H_1 and H_2). For this purpose, the horizontal components were first rotated in the plane of maximum energy to obtain the component H_{max}. The components Z and H_{max} were then rotated in the vertical plane, assuming lateral effects as negligible (this approximation was supported by the results provided by other surface seismic lines). In this way we obtained the radial R and transverse T signals for the VSP recorded at 266, 449 and 939 m offset.

In the multi-offset VSP analysis, the full-waveform real data - i.e., the total field before wavefield separation - were compared to numerical modelling results to improve the geological model information (Figure 8). Numerical synthetic signals (Z and H components) were calculated using a 2D viscoelastic finite-difference (FD) code. The source (vertical force) was a Ricker wavelet with 30 Hz peak frequency. The signal propagation was 2 s, with output-time sampling rate 1 ms. To account for velocity variations in the overburden composed of loose sediments (sand/clay) and basinal marly sediments, vertical-transverse isotropy (VTI) was assumed for the model. Anisotropy was estimated and added to the model in the depth range 390 - 600 m using the $\varepsilon = 0.1$ as Thomsen's parameter (Thomsen, 1986).The anisotropy parameter was tuned by analysing the direct signals in the real and synthetic data with offset, by minimization of the error energy. The analysis of the direct arrivals was done using the Z, R and T components obtained after signal orientation. The signals of the corresponding synthetic model used for comparison were also rotated in the radial and transverse directions. The real signal was interpreted and compared to the result of the synthetic model, which was tuned to obtain the minimization of the error energy in the measured (picked) travel times at corresponding offsets and depths. Figure 9 shows the result of the travel time comparison for the near-offset and for all the offset VSPs for both direct (Fig. 9a) and converted (Fig. 9b) waves. The analysis, including anisotropy and attenuation in the calculation of the synthetic data, allowed us to calibrate local velocity, interpreting and picking corresponding signals, and to tune the model at depth using the large-offset data to estimate a velocity variation at lateral distance from the well of approximately 300 m in the carbonate layers (Figure 10). Figure 10 shows (a) the preliminary estimated model which was used to calculate the synthetic signals in Fig. 8, (b) the Vp and Vs velocity profiles at 200 m offset and (c) the ray paths for direct PP transmitted arrivals at the limestone interface at about 600 m depth using the model depicted in Fig. 10a.

Beside analysis with direct arrivals, the rotated signals were used to interpret the converted components, and to estimate local shear-velocity variations (Figure 8b). The analysis shows that the observed data – as we can expect for a fractured formation filled by fluids – cannot be explained by assuming a Poisson medium (Eberhart-Philips et al., 1995). Figure 8b shows different offset VSP components and the corresponding synthetic signals. The transmitted converted PS waves are clearly interpretable in the transverse components (the T components calculated using the direct arrival). The travel-time comparison for converted waves is shown in Figure 9b, for the offset VSPs. Assuming a Poisson's medium, we observe large differences between the real and the calculated synthetic times (left bottom). We modeled and analysed these signals to determine the appropriate V_P/V_S ratio, taking into account the variation in the transmitted PP and PS travel paths, as shown in Figures 8a and 8b. This provides V_P/V_S information useful to characterize the local rock properties, and assess the presence of fluids and fractures associated to higher V_P/V_S ratio (Eberhart-Philips et al., 1995) in the proximity of the borehole. Finally, the offset VSP data were processed to obtain a multi-offset depth section and reflection imaging. For this purpose the rotated up- and down-going wavefields were separated and deconvolved. We used the transverse component to obtain images of the reflection section. Figure 11a shows the result of the multi-offset signal processing, compared and superimposed to the surface seismic section G13 (Della Vedova et al., 2013) passing through the well, time migrated data. The VSP signal improves the identification and resolution of the local structures near the well and characterizes dipping events interpretable in the seismic section. In Figure 11b we see the multi-offset CDP transform represented in depth, with the interpretation of the structural features in the reservoir at the well location, compared to the Vp/Vs ratio estimated at 200 m offset from the well.

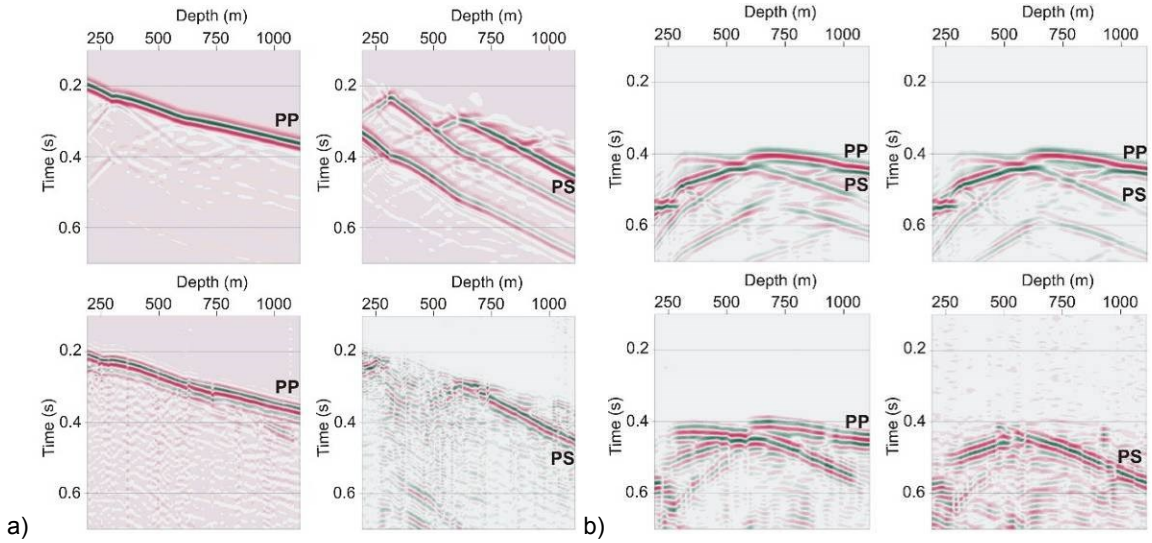

Figure 8: a) VSP at 266 m offset. On the left: synthetic (top) and real (bottom) radial R signals. On the right: synthetic (top) and real (bottom) transverse T signals. b) VSP at 939 m offset. Synthetic H direct and converted waves calculated with Poisson (top left) and higher Vp/Vs ratio (top right), and real (bottom) rotated R and T signals (modified after Poletto et al., 2013). PP and PS are transmitted waves, respectively direct and converted ones.

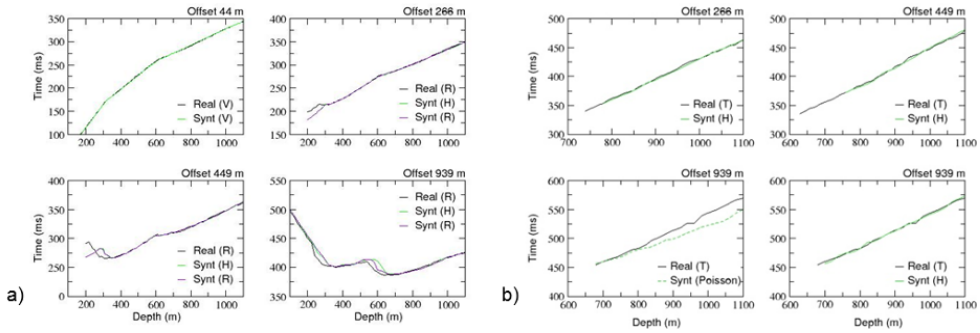

Figure 9: a) Analysis of direct-arrival travel times in synthetic and real data for the four VSP of the survey. From left top to right bottom: curves of the near offset, 266 m, 449 m and 939 m offset VSP. Matching of the curves is good for all the offsets. b) Comparison of real and synthetic arrival times for converted waves using a Poisson medium (left bottom) and after tuning Vp/Vs.

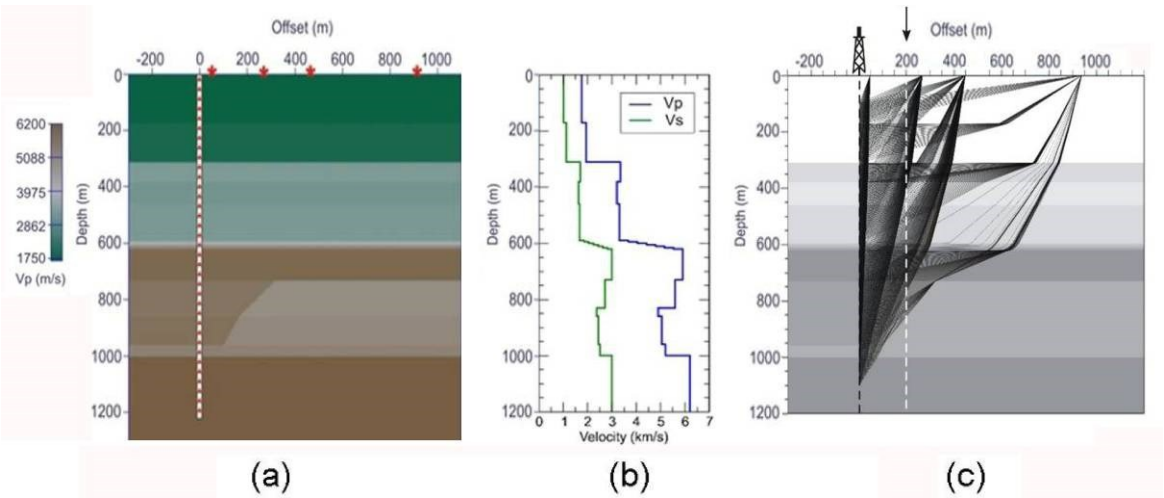

Figure 10: a) Preliminary velocity model estimated by error-energy minimization of the offset VSP travel times of Fig. 9. b) Velocity profiles at 200 m offset, shown by the arrow in Fig. 10c. c) Ray paths for direct PP transmitted arrivals at the limestone interface at about 600 m depth in the model of Figure 10a.

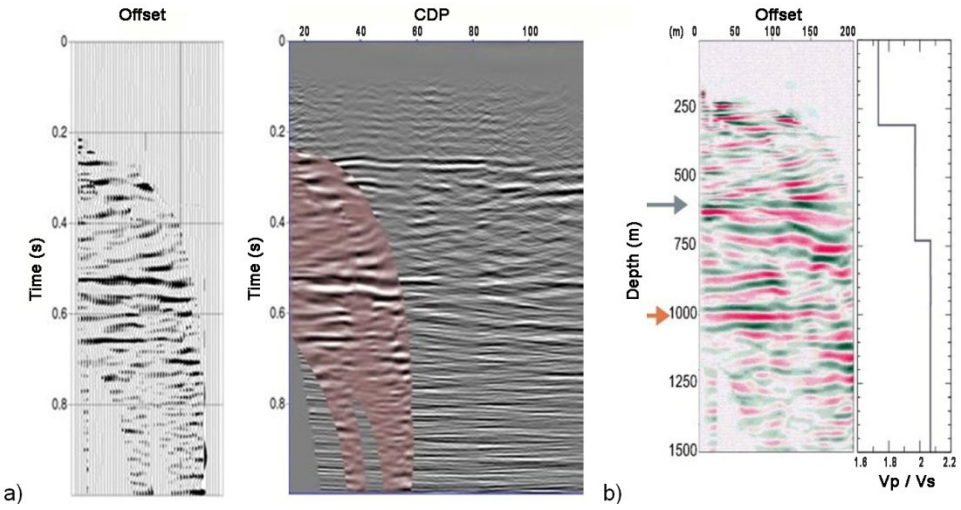

Figure 11: a) Multi offset VSP *time* section, compared (left) and superimposed (right side) to the seismic line G13 passing through the well. b) Multi-offset VSP *depth* section, showing structural features in the proximity of the well, with the interpretation of main changes in the carbonate platform. The grey and the orange arrows indicate respectively the top of the Paleogene and the top of the Mesozoic carbonate platform encountered in the well. The right panel shows the Vp/Vs ratio curve calculated at 200 m offset.

3.4 Bouguer gravity

The horizontal gradient of the Bouguer gravity anomaly (Cordell, 1979) was used to map structural lineations and to perform a 3D characterization, starting from 2D information given by the seismic lines. The axis of the major gravity anomalies (Fig. 12) likely correspond to the segments of the frontal Dinaric thrust system, NW-SE oriented, which are bounded by orthogonal strike-slip transfer faults.

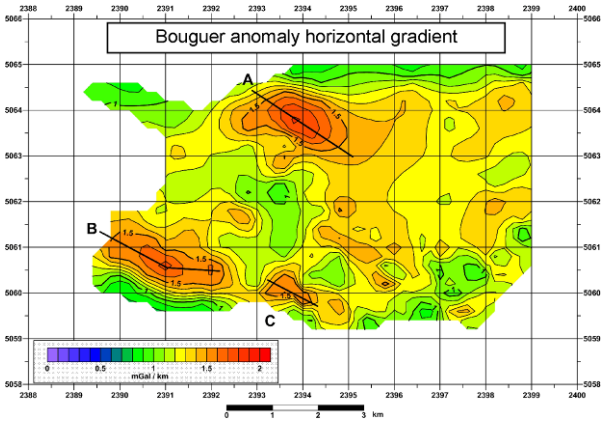

Figure 12: Bouguer anomaly horizontal gradient map. The axis of major gravity anomalies are indicated by black line and labelled (A, B and C).

The joint data interpretation allows us to recognize the fractured area that represents favourable geologic conditions for drilling and provides the most informative image of the lateral heterogeneity in the mass distribution at the depth of the reservoir and cap rock units, beneath the Grado Island. These structural features (Fig. 12) are interpreted as faulted segments of the distal Dinaric thrust front (Cimolino et al., 2010). The Grado-1 well is located to the SW of C gravity anomaly, whereas Grado-2 borehole is located to the NE of the same anomaly.

4. PRELIMINARY RESULTS FROM THE 2ND BOREHOLE

The second borehole was located downtown Grado (Figures 1), on the base of the results of the geophysical investigations, compatibly with the open space availability for the drilling site and the urban planning. The loose Plio-Quaternary sediment cover was drilled in April 2014 using a reverse rotary drilling system to reduce the drilling fluids invasion into the freshwater aquifers. N80 grade 13”3/8 casing was cemented in the Pliocene sediments (marls and sandstones bedrock down to 260 m depth). The rock bit 12”1/4 drilling phase started in late May 2014 using a Corsair 300 PDB drilling rig. At the end of May 2014, drilling was underway at about 450 m depth, within the Alpine molasse formation.

Borehole geophysics, interference test measurements between the two wells located at distance of approximately one kilometre, and 3-D thermo-fluid dynamic numerical modelling will be carried out to optimize the production and fluid re-injection, to design the heat exchangers for the public buildings, and to manage the sustainability of the geothermal plant.

5. THERMO FLUID-DYNAMIC MODELLING

We performed numerical thermo-fluid dynamic simulations (COMSOL 4.3a), as a support tool for the drilling of the second well and for the final design of the district heating system (Marcon, 2012). We evaluated and compared the performance of the geothermal doublet, also by inverting the flow between the production and re-injection wells. For this purpose the available geological and geophysical data were integrated into a simple conceptual model with the objective of (i) assessing the influence of the heterogeneities in the physical properties and the impact of the different boundary conditions on the model of the pressure and temperature fields, (ii) preliminarily assessing the reservoir energy production potential, and (iii) evaluating the response to production and re-injection of fluids over different time periods.

To make a realistic estimate of the reservoir energy production potential and to monitor reliable scenarios of the production capacity over time, these simulations will be adequately calibrated using the results of the logging, pumping and interference tests planned for late 2013, after the completion of the second borehole (Den Boer, 2008; Wong et al., 2012). The simulation domain (Fig. 13) of the confined fractured aquifer starts from the top of the carbonate aquifer at about 600 m depth. The horizontal model dimensions are 7 x 4 km and the two vertical wells are located 1 km apart; the vertical model dimension is 2.9 km; the capping formations were assumed impermeable and not included in the model; the production and the re-injection wells enter into the geothermal reservoir 500 and 600 m, respectively.

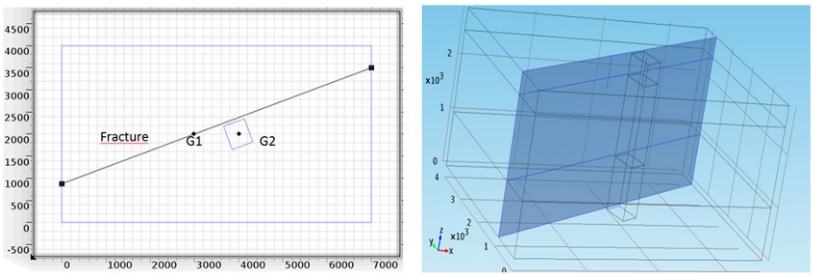

Figure 13: Plane (left) and 3-D view (right) of the simulation volume. The two wells Grado-1 and Grado-2 (G1 and G2 respectively) are in the central part of the domain; the diagonal plane indicates the fracture location. The prism centered on G2 borehole represents the aquifer portion of unknown permeability controlling the water flow between the well and the fracture.

The heat flow entering at the base of the model was calibrated using the Grado-1 well temperature data (Fig. 14), assuming a constant heat flow (45 mW/m^2) through time. The equilibrium geotherm is monitored by two temperature sensors (Pt 100) cemented at 450 and 695 m depth, respectively, on the outer steel casing.

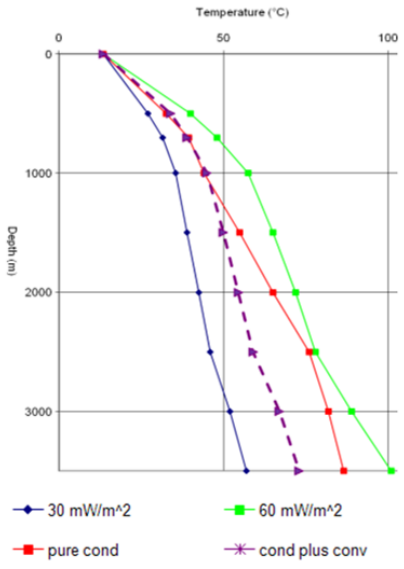

Figure 14: Sensitivity analysis and calibration of the vertical temperature distribution, with different basal heat flow inputs (30 and 60 mW/m2), assuming pure conduction (red line), or conduction plus convection (shown with purple dashed line), as supported by the experimental measurements down to 1100 m in Grado-1 well.

The open and diffuse network of fractures, represented by the active Dinaric and Anti-Dinaric thrust and fault systems interesting the carbonate reservoir, is the most crucial feature responsible for the onset and duration of the fluid circulation in the hydrothermal system. The fault system was conceptually simulated by an equivalent single vertical fault passing through the westernmost well (as encountered during drilling and confirmed by the seismic and gravity results) and assumed to be at an arbitrary distance of about

350 m from the second borehole (Grado-2). The unknown hydraulic resistance of the formation interposed between the reinjection borehole and the major fault directly controls the hydraulic shortcut between the two wells and substantially controls the heat exchange rate between rocks and moving fluids in the aquifer. The permeability parameter of this prism centered on the reinjection well requires to be calibrated with pumping and hydraulic interference test measurements. The values used for the physical properties of rocks, fluids and fracture and for the hydraulic and thermal boundary conditions are summarized in Table 1. In these initial tests, the equilibrium steady state temperatures at 1.5 and 3.5 km depth were estimated to be 50-55 °C and 74-78 °C, respectively, on the base of the experimental temperature measurements in Grado-1 well and of the preliminary geochemical analyses of the geothermal fluids (Petrini, pers. communication).

Transient simulations were obtained by assuming a geothermal water production of about 0.030 m^3/s ($110x10^3$ Kg/h) and a difference of temperature between production and re-injection fluids of 20 °C.

Table 1: Values for the physical properties of various materials and for the hydraulic and thermal boundary conditions used in the thermo-fluid dynamic modeling. Water values refer to seawater in lab conditions.

Physical Property	Modelling values	Boundary Condition	Assumed value
Water dynamic viscosity	0,001 Pa·s	Upper boundary T condition	39 °C
Water heat capacity	3925 J/kg/°C	Re-injected fluid temperature	25 °C
Water density	1025 kg/m3	Basal heat flux	45 mW/m2
Matrix porosity	0,05	Undisturbed water pressure	300 kPa
Fracture porosity	0,3	Pumping/injection rate	0,030 m^3/s
Reservoir heat capacity	950 J/kg/°C		
Reservoir rock density	2700 kg/m3		
Reservoir rock permeability	1 mD (10-15 m2)	**Simulation time period**	
Vertical prism permeability	100 mD	1,5·109 s (50 a)	
Fracture permeability	500-1000 mD		
Fracture thickness	0,05 m		

These values correspond to 2.4 MWt nominal power production potential, which would imply about 4.000 MWh of thermal energy over a period of six months at maximum load. These simulations allowed us to evaluate the strong influence of the fracture network permeability (Wong et al., 2012), for which we used values between 500 and 1000 mD, and to preliminarily assess the hydraulic and thermal sustainability of the district heating system over 50 years. Figure 16 shows the steady-state pressure field around the pumping and re-injection wells. The white lines represent the flow lines, the black arrows are the flow vectors within the fracture.

The colored envelops around the production and re-injection wells represent the isopressure surfaces, plotted with values in bars, according to the palette to the right. This simulation shows as the fracture acts as a preferential channel draining water also from the highly resistive carbonate formation (Wong et al., 2012).

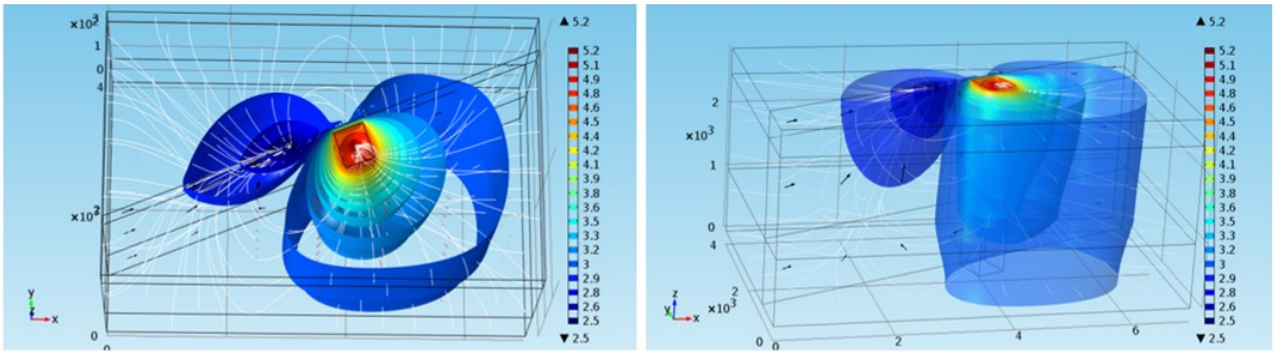

Figure 15: Vertical and lateral axonometric view of the steady-state pressure field around the production and re-injection wells.

The planned down-hole investigations and cross-well interference tests shall allow to design the heat exchangers and to choose the most adequate management parameters in order to guarantee an economic and sustainable use of the Grado geothermal resource.

6. CONCLUSIONS

The seismic and gravity surveys carried out in the Grado Island and surrounding lagoon constitute a fundamental tool for the potential assessment of the Grado geothermal resource, and for the completion of the district-heating system planned for the public buildings of the city. The integration of the new geophysical data with the previous Grado-1 site-survey and well data allowed us to define the major structural features characterizing the confined carbonate reservoir and to locate the second well of the geothermal doublet at the crossing between G12 and G13 seismic lines.

The analysis of the full waveform offset VSP signals and of viscoelastic synthetic signals (including anisotropy), integrated with lateral seismic imaging, improved the characterization of the geothermal reservoir coherent with the available geological and geophysical data. The results include the recognition of changes in the elastic rock properties within the reservoir formations obtained using the converted components to estimate the VP/VS ratio. The results suggest significant lateral changes both in the over-burden terrigenous formations and in the carbonate geothermal reservoir, as expected at the active Dinaric deformation front. The Grado-1 well is located on the frontal Dinaric thrust likely interested by strike-slip transfer faults with anti-Dinaric direction (NE-SW), as suggested by the regional tectonic reconstruction and by the seismic and gravity investigations. This network of fractures and the associated deformation was locally imaged to the east of Grado-1 well by borehole seismic investigations. The results highlight the main features of the geothermal reservoir and of the cap rock formations belonging to the outer Dinaric thrust front (Cimolino et al., 2010). The open and diffused network of fractures and strike-slip transfer faults with anti-Dinaric direction (NE-SW) is the most crucial feature responsible for the onset and duration of the fluid circulation in the hydrothermal system.

We used this information to constrain the conceptual model, physical properties and boundary conditions of a preliminary 3-D thermo-fluid dynamic numerical modelling, including the presence of a fracture system. The simulations allowed us to evaluate the coupling of the production/re-injection wells and the strong influence of the permeability of the fracture network, which acts as a preferential drain, and to assess in a preliminary way the geothermal potential and the long-term sustainability of the district heating system.

The Grado-2 borehole, the well logging and the hydraulic measurements will be completed by June 2014, allowing the calibration of the numerical simulations, assess the production capacity and tune the long turn sustainability.

ACKNOWLEDGEMENTS

We thank the Grado Administration for the field support and for the permission to present the results. Thanks are due to all OGS crew who took part in data acquisition; Gualtiero Böhm for his help in the preparation of ray tracing and modelling results, and Giorgia Pinna for the calculation of the attenuation by log data and VSP. Thanks also to Prof. Riccardo Petrini for the geochemical analyses and fruitful discussion on geothermal fluids.

REFERENCES

AGIP: Temperature Sotterranee. Inventario dei dati raccolti dall'AGIP durante la ricerca e la produzione di idrocarburi in Italia, *Fratelli Brugora*, Segrate, Milano, (1977).

AGIP: Aggiornamenti Temperature Sotterranee – Pozzi a Terra, (1986).

AGIP: Acque dolci sotterranee. Inventario dei dati raccolti dall'AGIP durante la ricerca di idrocarburi in Italia dal 1971 al 1990, *Graf 3 Roma*, (1994).

Banerjee B., Das Gupta S.P.: Gravitational attraction of a rectangular parallelepiped, *Geophysics*, vol. 42, n° 5, (1977), 1053-1055.

Barnaba P.F.: L'anomalia geotermica della Bassa Pianura Veneto-Friulana, Acque sotterranee, n° 74, (2001), 33-39.

Bellani S., Calore C., Della Vedova B., Grassi S., Marson I., Nicolich R., Perusini P., Squarci P.: Valutazione di dettaglio delle strutture profonde della Bassa Pianura Friulana, Inventario delle risorse geotermiche nazionali, Ministero Industria, Comm., Art., *STAR-C.N.R.*, Tav. 19, (1994).

Blias, E.: Accurate interval Q-factor estimation from VSP data, *Geophysics*, **77** (3), (2012), WA149– WA156.

Calore C., Della Vedova B., Grassi S., Marson I., Nicolich R., Squarci P.: A hydrotermal system along the Coastal Area of Friuli-Venezia Giulia Region (NE Italy), *Proceedings of the World Geothermal Congress*, Florence, n° 2, (1995), 1269-1274.

Cassano E., Anelli L., Fichera R., Capelli V.: Pianura Padana. Interpretazione integrata di dati geofisici e geologici, *73° Congr. Soc. Geol. It*, (1986).

Cati A., Sartorio D., Venturini S.: Carbonate platforms in the subsurface of the Northern Adriatic Area, *Mem. Soc. Geol. It. 40*, (1987), 295-308.

Casero P., Rigamonti A., Iocca M.: Paleogeographic relationship during Cretaceous between the Northern Adriatic area and the Eastern Southern Alps, *Mem. Soc. Geol. It. 45* (1990), 807-914.

Cimolino A., Della Vedova B., Nicolich R., Barison E., and Brancatelli G.: New evidence of the outer Dinaric deformation front in the Grado area (NE-Italy), *Rendiconti Lincei*, vol. 21, supplement 1, (2010), 167-179.

Cordell, L.: Gravimetric expression of graben faulting in Santa Fe Country and the Espanola Basin, New Mexico, *New Mexico Geol. Soc. Guidebook*, 30th Field Conf., (1979), 59-64.

Della Vedova B., Marson I., Palmieri F.: Gravity study of a low enthalpy hydrothermal area: Grado Lagoon–NE Italy, *European Geophysical Society–XIII General Assembly*, Annales Geophysicae, Special Issue, (1988).

Della Vedova B., Castelli E., Cimolino A., Vecellio C., Nicolich R., and Barison E.: La valutazione e lo sfruttamento delle acque geotermiche per il riscaldamento degli edifici pubblici, *Rassegna Tecnica del Friuli Venezia Giulia 6*, (2008a), 16-19.

Della Vedova B., R. Nicolich, Castelli E., Cimolino A., Vecellio C., Barison E.: The geothermal potential of the carbonatic platform buried beneath the Veneto and Friuli coastal areas: preliminary results from the Grado-1 borehole (NE Italy), *Proceedings of the 70th EAGE Conference & Exhibition*, Workshop 9: Geosciences for the Geothermal Exploration: an integrated approach, Rome, (2008b), 16-19.

Della Vedova, B., Petronio, L., Poletto, F., Palmieri, F. and Marcon, A.: Reservoir characterization for the completion of the geothermal district heating system in Grado (NE Italy), *Proceedings of the European Geothermal Congress 2013*, Pisa, Italy, (2013), *in press*.

Den Boer C.A.: Doublet Spacing in the "Delft Aardwarmte Project", BSc thesis report, TU Delft, (2008).

Eberhart-Philips, D., Stanley, W. D., Rodriguez, B. D. and Lutter, W. J.: Surface seismic and electrical methods to detect fluids related to faulting, *Journal of Geophysical Research*, **100**, no. B7, (1995), 12919–12936.

Fantoni R., Castelli D., Merlini S., Rogledi S., Venturini S.: La registrazione degli eventi deformativi Cenozoici nell'avanpaese Veneto-Friulano, mem. Soc. Geol. It., n °57, (2002), 301-313.

Fantoni R., Della Vedova B., Giustiniani M., Nicolich R., Barbieri C., Del Ben A., Finetti I., Castellarin A.: Deep seismic profiles through the Venetian and Adriatic foreland (Northern Italy), *Memorie di Scienze Geologiche 54*, (2003), 131-134.

Grassi S.: Alcune osservazioni sulle caratteristiche geochimiche delle acque sotterranee della Bassa Pianura Friulana, *Atti Soc. Tosc. Sci. Nat.*, *Memorie*, Serie A, (1994), 1-15.

Hauge, P. S.: Measurements of attenuation from vertical seismic profiles, *Geophysics*, **46** (11), (1981), 1548–1558.

Hinze W.J. et al.: New standards for reducing gravity data: The North America gravity database, *Geophysics*, vol. 70, n° 4, (2005), J25-J32.

Marcon A.: Progetto di teleriscaldamento geotermico di Grado (GO): valutazione della sostenibilità della risorsa tramite simulazioni numeriche, tesi specialistica, Università di Trieste, (2012).

Marson I., Morelli C.: A microgravimetric network for studying local gravity variations in North-eastern Italy (Friuli) connected with earthquake activity: institution of the net, *Bollettino di Geodesia e Scienze Affini*, vol. XXXVIII n°2, (1979), 345-360.

Nicolich R., Della Vedova B., Giustiniani M., Fantoni R.: Carta del Sottosuolo della Pianura Friulana (Map of Subsurface Structures of the Friuli Plain), Regione Autonoma Friuli Venezia Giulia, Direz. Centrale Ambiente e Lav. Pub., *Servizio Geologico*, *Note Illustrative*, Tav. 4, (2004).

Petronio L., Poletto F., Palmieri F. and Della Vedova B.: Geophysical investigations of the Grado deep structures (NE Italy) for the location of the second geothermal borehole, *G.N.G.T.S. 31° Convegno Nazionale*, Sessione 3.1, (2012), 28-33.

Poletto F., Corubolo P., Farina B., Schleifer A., Petronio L. and Della Vedova B.: Multi-offset VSP for the integrated geophysical characterization of the Grado (NE Italy) carbonatic reservoir. *Proceedings of the European Geothermal Congress 2013*, Pisa, Italy, (2013).

Sun, F. L., Milkereit, B. and Schmitt, D. R.: Measuring velocity dispersion and attenuation in the exploration seismic frequency band, *Geophysics*, **74** (2), (2009), WA113–WA122.

Thomsen, L.: Weak elastic anisotropy, *Geophysics*, **51** (10), 1954-1966, (1986).

Venturini S.: Il pozzo Cargnacco 1: un punto di taratura stratigrafica nella pianura friulana, "*Memorie della Società Geologica Italiana*", 57, (2002), 11-18.

Wong L. W., Blocher G., Kastner O., Zimmermann G.: Multiphysics between Deep Geothermal Water Cycle, Surface Heat Exchanger Cycle and Geothermal Power Plant Cycle, *Comsol Conference 2012*, Milan, (2012).